3Dp1-10L
(Late-News Paper)

Touch Detection Using Scattering Light on Palm in an Aerial Guide with AIRR

Kengo Fujii[1], Kazunari Chiba[1], Ikuya Saji[1], Masaki Yasugi[1,2], Hirotsugu Yamamoto[1,2]

k_fujii@yamamotolab.science
[1] Utsunomiya University, 7-1-2, Yoto, Utsunomiya, Tochigi, 321-0904, Japan.
[2] JST ACCEL, 7-1-2, Yoto, Utsunomiya, Tochigi, 321-0904, Japan.
Keywords: aerial image, AIRR, touch detection, aerial interface

ABSTRACT

This paper proposes a method for touch detecting on a guide illumination formed by aerial imaging by retro-reflection (AIRR). Touch detection is performed from the intensity of scattered light generated by the contact with an aerial image formed parallel to the aperture surface of AIRR.

1 INTRODUCTION

In recent years, the use of masks, hand disinfection, and other hygiene risks have been daily performed. We focus on contact, which is one of the sanitation problems, and propose an aerial button that can be operated without contact. Our proposed aerial button is operated by touching an aerial guide with aerial imaging by retro-reflection (AIRR). AIRR is an aerial-image-forming technique [1]. International standardization of aerial display technology has been in progress recently, and it is expected to become more common [2]. Aerial guides are studied to guide non-contact hand vein imaging [3]. In Non-contact vein imaging, there is no physical guide to guide the user to the sensor area. An aerial guide can be used to guide the user without physical contact. This makes the button hygienic, as no physical contact occurs. Replacing buttons that are operated by an unspecified number of people, such as elevator buttons, with aerial buttons will reduce the hygiene risk.

In this paper, we investigate a contact detection method using scattered light generated when a user touches an aerial guide formed by AIRR, using simulations.

2 PRINCIPLE

2.1 Aerial Imaging by Retro-Reflection (AIRR)

Fig. 1 shows an aerial image formed with AIRR. Fig. 2 shows the principle of AIRR. This setup consists of a light source, a beam splitter, and a retro-reflector. The beam splitter reflects rays from the light source. The reflected rays are retro-reflected, that is, reflected reversely at the incident positions on the retro-reflector. The retro-reflected rays are converged to the position of the plane-symmetrical of the light source with respect to the beam splitter.

Fig. 1 Aerial image formed with AIRR (aerial imaging by retro-reflection)

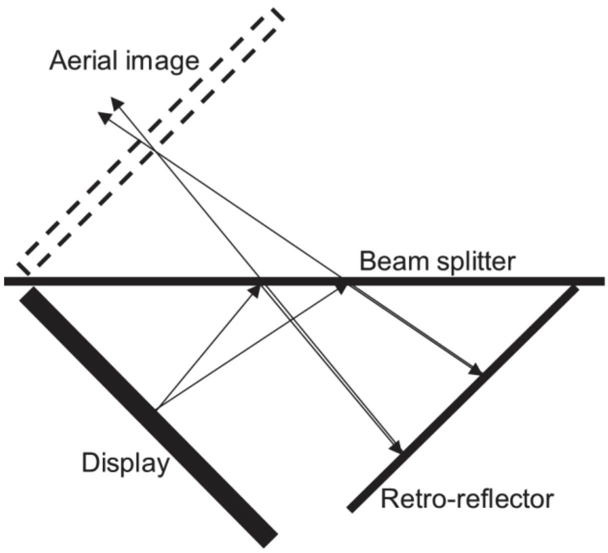

Fig. 2 Principle of AIRR

2.2 Aerial Guide Formed with AIRR

Fig. 3 shows the principle of the aerial guide formed with AIRR. The retro-reflector is arranged in surround the light source. In aerial guide by AIRR, the aerial guide is formed on parallel to the aperture plane of the AIRR. The principle of aerial imaging is the same as the conventional AIRR. however, this method has a wider viewing angle than the conventional AIRR.

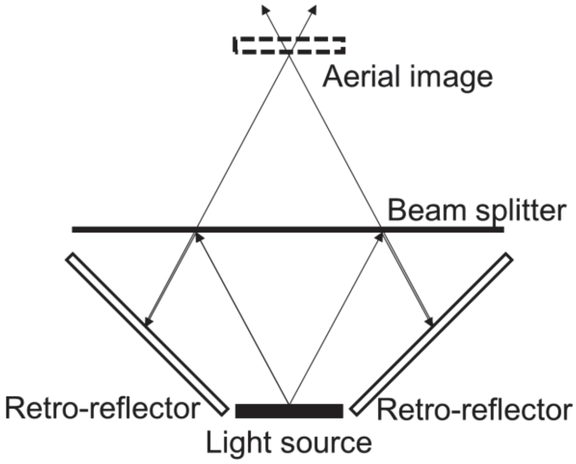

Fig. 3 Principle of an aerial guide formed with AIRR

2.3 Touch Detection on an Aerial Guide Formed with AIRR

Fig. 4 shows the principle of touch detection on an aerial guide formed with AIRR. We propose a method that uses scattered light to detect the user's touch on an aerial image. AIRR images the light from the light source in a plane-symmetrical by a beam splitter. Therefore, when the user's palm is placed in the imaging position of the aerial image, scattered light is generated on the palm. To observe the scattered light, a photodetector is used in the optical system. As shown in Fig. 4, the scattered light is detected by a photodetector through the beam splitter.

However, in addition to the scattered light from the palm, two types of noisy light are also detected by the photodetectors.

The first is the light that comes out of the light source, is reflected by the beam splitter, and then directly enters the photodetector. This light is detected even when it does not touch the aerial image. Therefore, it can be removed by treating it as an offset of the detected value.

The second is the scattered light generated in the palm by the light transmitted through the beam splitter from the light source. It is difficult to distinguish this light from the scattered light generated by the aerial image. Therefore, it is necessary to perform correct touch detection including this light.

3 RESULTS

We simulated ray tracing to confirm that the light scattered in the palm could be used for detection. We used Lighttools 9.0 for ray tracing.

Fig. 5 shows the parameters of the simulation model. In this simulation, the size of the light source and the beam splitter are fixed. In addition, the distance between the light source and the beam splitter is fixed. The size of the scatterer is variable and the scattering at the surface is Lambert. The distance between the scatterer and the beam splitter is varied. The size of the photodetector is variable and it detects the light entering the surface facing the scatterer.

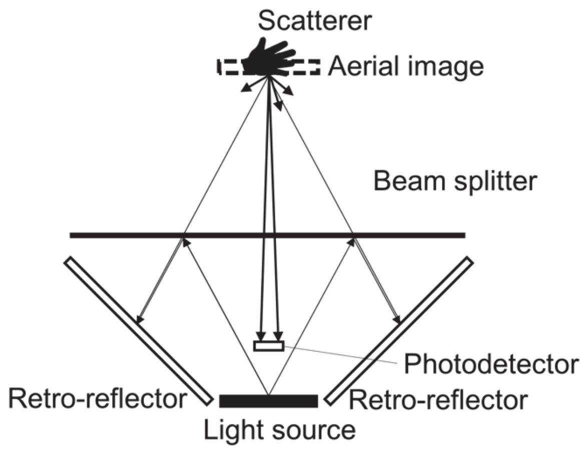

Fig. 4 Principle of touch detection on an aerial guide formed with AIRR

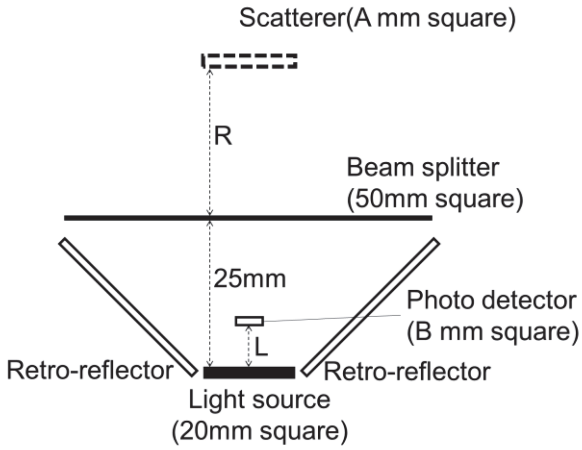

Fig. 5 Parameters of the simulation model

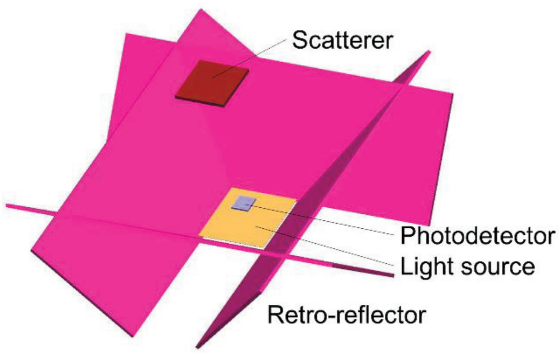

Fig. 6 Simulation model of optical systems

Fig. 6 shows an example of a simulation model. The detection values of the photodetector were obtained by simulation while varying each parameter.

Fig. 7 shows an example of results from a ray tracing.

3.1 Simulations of Some Positions of a Scatterer

First, we simulated the case where the scatterer (palm) is moving back and forward from the position of the aerial image.

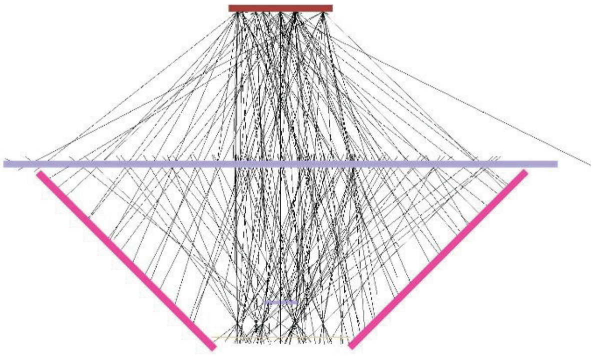

Fig. 7 Example of a result from a ray tracing

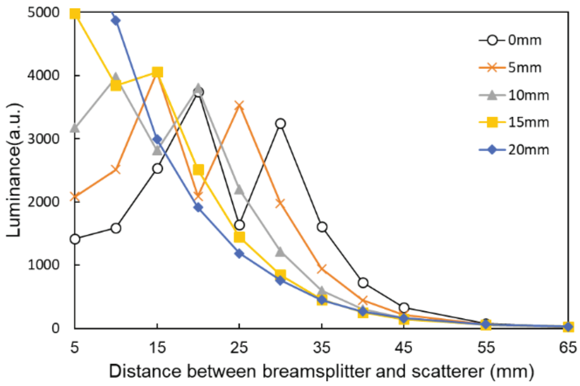

Fig. 8 Relationships between the distance of the scatterer and the photodetector at the distance between the light source and the photodetector

Fig. 8 show the relationships between the distance of the scatterer and the photodetector at the distance between the light source and the photodetector. Fig. 9 show examples of results from a ray tracing.

When comparing the peaks of each result, the peak point where the position of the aerial image and the scatterer coincides (25 mm) was found at a distance of 5 mm between the light source and the photodetector. For other distances, the peak point was shifted. As a result, we found that the distance between the light source and the photodetector needs to be set appropriately for touch detection.

On the other hand, when the distance between the light source and the photodetector is other than 20 mm, there are two peak points. The photodetector also observes the scattered light transmitted from the light source through the beam splitter to the scatterer. For this reason, the peak of scattered light which is not retro-reflected light is considered to be detected.

When the distance between the light source and the photodetector was 20 mm, there was no peak of scattered light due to retro-reflected light. The distance between the light source and the photodetector should be as close to the light source as possible.

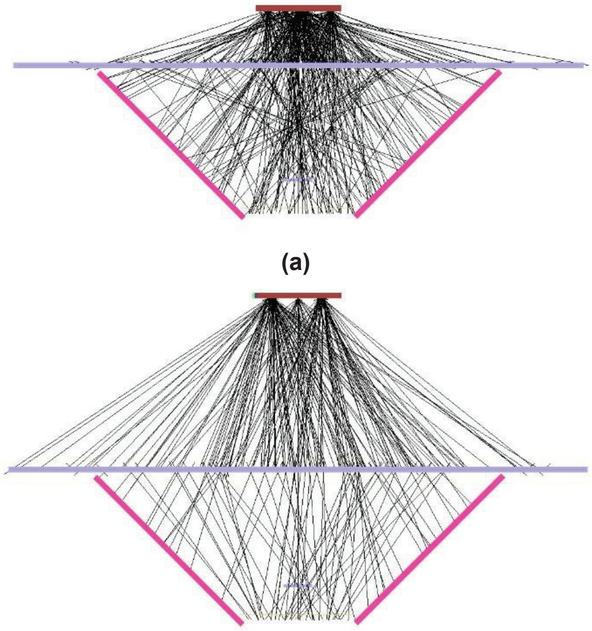

(a)

(b)

Fig. 9 Results of ray-tracing simulations for (a) 10 mm and (b) 30 mm distance between the beam splitter and the scatterer

Next, we performed simulations for different scatterer sizes. The position and size of the photodetector are fixed. Fig. 10 show the relationships between the position of the scatterer and the photodetector's detection values at each scatterer size. Fig. 11 show examples of results from a ray tracing. The size of the scatterer was simulated from half to 1.5 times the size of the aerial image. The simulation results show that the obtained detections had similar peak values regardless of the size of the scatterer. However, the peak value becomes smaller as the scatterer is smaller. In other words, the smaller the palm size in relation to the size of the aerial image, the lower the peak value. Accordingly, for accurate touch detection, the size of the aerial guide has to be determined for the small palm of the expected user.

3.2 Simulations of Some Positions of a Photodetector

Finally, we simulated a case in which the scatterer (palm) was fixed at the position of the aerial image and the position of the photodetector was moved. 7 patterns of photodetector size were verified for each 2.5 mm edge length. Fig. 12 show the relationships between the distance between the light source and the photodetector and the detection values of the photodetectors at different photodetector sizes. Fig. 13 show examples of results from a ray tracing. The larger the photodetector, the more light it detects. On the other hand, a loss of light is generated in the aerial image because the light source is obscured. In addition, the detection value of the scattered light due to non-reflected light decreases. Here, the former decreases when the photodetector is close to the light source, and the latter decreases when the photodetector is far from the light source. As a result, when the photodetector size is 2.5 mm square, the peak value is at a distance of 5 mm from the light source, but the peak value disappears when the photodetector size is 17.5 mm square. These results show that the smaller the size of the photodetector and the closer its position is to the light source, the larger the peak value appears.

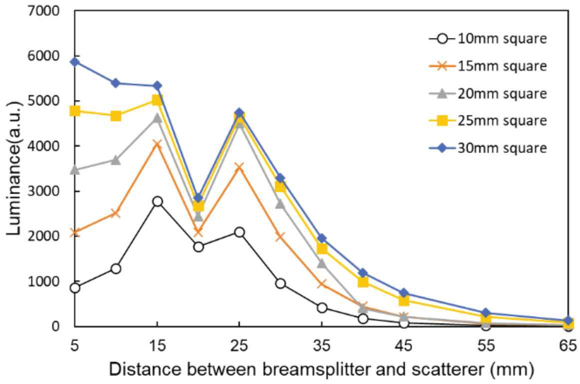

Fig. 10 Relationships between scatterer positions and photodetector detections at different photodetector sizes

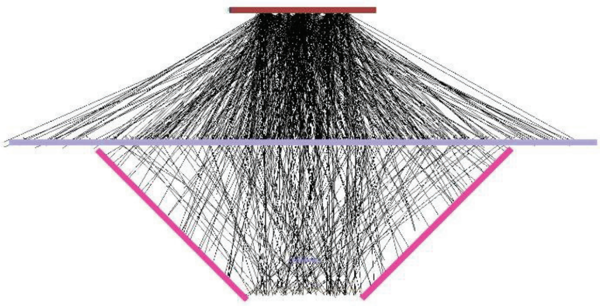

Fig. 11 Simulation result for a 2.5 mm square photodetector

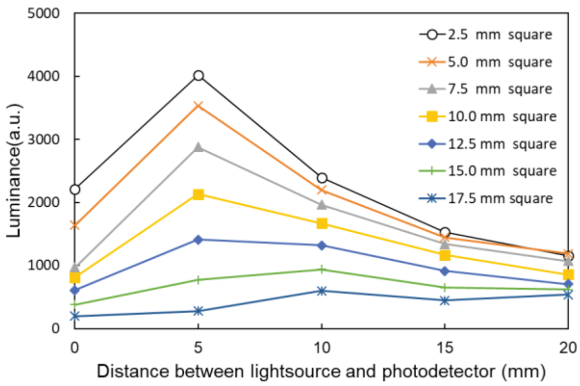

Fig. 12 Relationships between distance from the light source to the photodetector and the detection value of the photodetector at different sizes of photodetectors

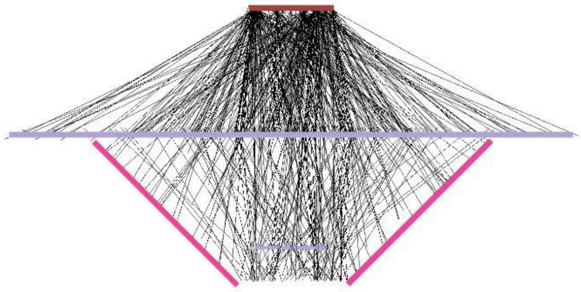

(a)

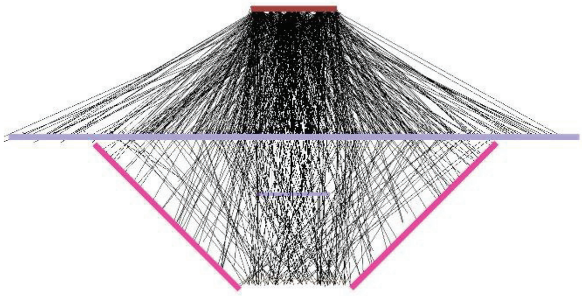

(b)

Fig. 13 Simulation results for 12.5 mm square photodetectors with (a) 5 mm and (b) 15 mm distances between the light source and the photodetector

4 CONCLUSION

Touch detection of an aerial guide using scattered light was verified by simulation. As a result, the necessity of setting the size of the aerial image to match the size of the palm and the relationship between the distance between the light source and the photodetector and the peak value were clarified.

A part of this work was supported by JST/ACCEL (grant no. JPMJAC1601) and JSPS KAKENHI (19H04155, 20H05702).

REFERENCES

[1] H. Yamamoto, Y. Tomiyama, and S. Suyama, “Floating aerial LED signage based on aerial imaging by retro-reflection (AIRR),” Opt. Express **22**, pp. 26919-26924 (2014).

[2] B. Javidi, A. Carnicer, J. Arai, T. Fujii, H. Hua, H. Liao, M. Martínez-Corral, F. Pla, A. Stern, L. Waller, Q. Wang, G. Wetzstein, M. Yamaguchi, and H. Yamamoto, "Roadmap on 3D integral imaging: sensing, processing, and display," Opt. Express **28**, pp. 32266-32293 (2020).

[3] I. Saji, K. Kawai, R. Kujime and H. Yamamoto, “Non-contact Hand Vein Imaging by Use of Aerial Guiding Illumination with AIRR,” Proc. IDW19’, pp. 1696-1699 (2019).